J. of Fire Prot. Engr., 5 (2), 1993, pp 39–52

COMPUTER MODELING OF COMPARTMENT FIRES

by

G. V. Hadjisophocleous and M. Cacambouras
National Fire Laboratory
Institute for Research in Construction
National Research Council of Canada
Ottawa, Canada K1A OR6

SUMMARY

A three dimensional computational fluid dynamics model for the simulation of fire is presented. The model solves the governing partial differential equations for continuity, momentum, and energy using the control volume formulation. Turbulence is modeled using the k-ε model and fire is described as a heat source.

The above model has been used to simulate fire inside an enclosure. The results of studies on the fire location, size of the compartment opening and existence of internal objects are presented. The predictions obtained are compared with experimental data and found to be in reasonable agreement.

INTRODUCTION

Mathematical modeling offers an economical and accurate approach for the prediction and study of fire and smoke spread. The fundamental conservation equations for heat, momentum and mass are solved numerically to simulate the evolution of fire and its characteristics. Two basic methodologies are used for fire simulation: zone and field modeling. In zone models, the fire room is divided into a number of zones, a hot upper layer and a cooler lower with uniform gas properties in each zone. Ordinary differential equations expressing conservation of mass and energy are applied to each zone and solved numerically. These equations employ empirical relationships and constants obtained from experiments, therefore, zone models can only be used for problems that lie within the range of experiments used to derive the equations[1]. On the other hand, field models, solve the fundamental partial differential equations for conservation of mass, momentum and energy numerically with minimum empiricism and therefore, they can be applied to a variety of problems with minor modifications.

A number of field models have been developed and used successfully for fire simulations. One of the first fire field models is JASMINE[2,3]. It is based on the commercial code PHOENICS and uses the semi-empirical k-ε model for turbulence and the eddy-dissipation concept to model combustion. The model was validated using experimental data and was applied to simulate fires in tunnels, hospitals and shopping malls[4,5].

Another field model used for fire simulation was developed by Ku, Doria and Lloyd[6]. It is based on the general two-dimensional model UNDSAFE and was used to predict 2-D flow in corridors. In this model, turbulence is approximated using an algebraic model. Measured floor temperatures were used as input to the computer runs. Two-dimensional flow in enclosures with a number of different thermal boundary conditions were accounted for successfully.

The model UNDSAFE was extended to 3-D by Satoh[7,8]. In this model, combustion is approximated by a heat source, linearized at the time beginning and no turbulent model is employed. The model was used to study flow in high-rise buildings and fire behaviour around windows and vertical exterior walls. Fires in aircraft cabins were also studied[9].

Hollen et al.[10] developed another field model, KAMELEON. This model uses the k-ε model for turbulence, the Discrete Transfer Model

for radiation and a soot model based on the eddy-dissipation concept combustion. The 3-D model was validated using experimental data for both compartment and pool fires. Stable calculations were performed for different combustion cases.

Another field model is FLOW3D, developed at HARWELL Laboratories, U.K.[11]. This model was used to simulate the King's Cross fire, predicting successfully the "trench effect" which was also observed experimentally.

Other field models for fire simulations have been developed by Morita, Oka and Hirota[12], Joh, Mashiege and Sugawa[13], Kaplan and Oran[14] and Chow[15].

The mathematical model presented in this work is being developed at the National Fire Laboratory of the Institute for Research in Construction, National Research Council of Canada (NRCC). The model is based on a computer model developed by Lai[16,17], specifically for the simulation of industrial furnaces and burners, as well as a 2-D model developed by Hadjisophocleous[18] for compartment fire simulations. Lai's model has been extensively modified so it can be used for room fire simulations following the procedures used in[18].

The objective of this work is the development and validation, using full scale experimental data, of a fire model that can be used for compartment fires, pool fires, fires in atria and fires in rooms with multiple obstacles. This paper presents some validation tests for compartment fires, as well as, results of a fire simulation in a room with an obstacle between the door and the fire.

Mathematical Model

The unsteady, turbulent free, convective flows and heat transfer resulting from fire in a compartment is modeled using the fundamental differential equations of mass, momentum and energy. Independent variables are the position (x, y, z) in cartesian coordinates and time. Dependent variables are the components of velocity (u, v, w), pressure P, enthalpy h, turbulent kinetic energy k, and energy dissipation rate ε. Auxiliary variables are the density of species ρ, effective viscosity μ_{ef} ($\mu_{ef} = \mu_l + \mu_t$ where μ_l is the laminar viscosity and μ_t is the turbulent viscosity), and temperature T (derived directly from the energy equation). These equations are:

Mass

$$\frac{\partial \rho}{\partial t} + \frac{\partial (\rho u)}{\partial x} + \frac{\partial (\rho v)}{\partial y} + \frac{\partial (\rho w)}{\partial z} = 0 \qquad (1)$$

Momentum (2)

$$\frac{\partial (\rho u)}{\partial t} + \frac{\partial (\rho uu)}{\partial x} + \frac{\partial (\rho uv)}{\partial y} + \frac{\partial (\rho uw)}{\partial z} = -\frac{\partial P}{\partial x} + \frac{\partial \tau_{xy}}{\partial x} + \frac{\partial \tau_{xy}}{\partial y} + \frac{\partial \tau_{xz}}{\partial z}$$

$$\frac{\partial (\rho v)}{\partial t} + \frac{\partial (\rho uv)}{\partial x} + \frac{\partial (\rho vv)}{\partial y} + \frac{\partial (\rho wv)}{\partial z} =$$

$$-\frac{\partial P}{\partial y} + \frac{\partial T_{yx}}{\partial x} + \frac{\partial T_{yy}}{\partial y} + \frac{\partial T_{yz}}{\partial z} - g(p - p_{ref}) \qquad (3)$$

(4)

$$\frac{\partial (\rho w)}{\partial t} + \frac{\partial (\rho uw)}{\partial x} + \frac{\partial (\rho vw)}{\partial y} + \frac{\partial (\rho ww)}{\partial z} = -\frac{\partial P}{\partial z} + \frac{\partial T_{zx}}{\partial x} + \frac{\partial T_{zy}}{\partial y} + \frac{\partial T_{zz}}{\partial z}$$

Energy (5)

$$\frac{\partial (\rho h)}{\partial t} + \frac{\partial (\rho uh)}{\partial x} + \frac{\partial (\rho vh)}{\partial y} + \frac{\partial (\rho wh)}{\partial z} = \frac{\partial q_x}{\partial x} + \frac{\partial q_y}{\partial y} + \frac{\partial q_z}{\partial z} + q_s$$

where

$$\tau_{xx} = \frac{2}{3}\mu_{ef}\left(2\frac{\partial u}{\partial x} - \frac{\partial v}{\partial y} - \frac{\partial w}{\partial z}\right)$$

$$\tau_{yy} = \frac{2}{3}\mu_{ef}\left(2\frac{\partial v}{\partial y} - \frac{\partial u}{\partial x} - \frac{\partial w}{\partial z}\right)$$

$$\tau_{zz} = \frac{2}{3}\mu_{ef}\left(2\frac{\partial w}{\partial z} - \frac{\partial v}{\partial y} - \frac{\partial u}{\partial x}\right)$$

$$\tau_{xy} = \tau_{yx} = \mu_{ef}\left(\frac{\partial u}{\partial y} + \frac{\partial v}{\partial x}\right)$$

$$\tau_{xz} = \tau_{zx} = \mu_{ef}\left(\frac{\partial w}{\partial x} + \frac{\partial u}{\partial z}\right)$$

$$\tau_{zy} = \tau_{yz} = \mu_{ef}\left(\frac{\partial w}{\partial y} + \frac{\partial v}{\partial z}\right)$$

$$q_x = -\mu_h \frac{\partial h}{\partial x}, \quad q_y = -\mu_h \frac{\partial h}{\partial y}, \quad q_z = -\mu_h \frac{\partial h}{\partial z}$$

$$\mu_h = \frac{\mu_l}{Pr_l} + \frac{\mu_t}{Pr_t}$$

q_s = the heat source

Pr_l = laminar Prandtl number $= \frac{\upsilon}{\alpha} = 0.7$

υ = laminar kinematic viscosity

α = thermal diffusivity

Pr_t = turbulent Prandtl number = 1.0

These equations can be written in the general form

$$\frac{\vartheta(\rho\Phi)}{\vartheta t}+\frac{\vartheta(\rho u\Phi)}{\vartheta x}+\frac{\vartheta(\rho v\Phi)}{\vartheta y}+\frac{\vartheta(\rho w\Phi)}{\vartheta z}=$$

$$\frac{\vartheta}{\vartheta x}(\Gamma_\Phi\frac{\vartheta\Phi}{\vartheta x})+\frac{\vartheta}{\vartheta y}(\Gamma_\Phi\frac{\vartheta\Phi}{\vartheta y})+\frac{\vartheta}{\vartheta z}(\Gamma_\Phi\frac{\vartheta\Phi}{\vartheta z})+S_\Phi \qquad (6)$$

where Φ represents the dependent variables, Γ the effective exchange coefficient of Φ and S_Φ the source terms.

Turbulence Model

To complete the set of equations, the stress terms and heat flux require a transport law. For the laminar case, this is covered by the usual molecular equations. But the fire phenomenon is turbulent in nature, and a turbulence model is needed. Because of its wide applicability and simplicity, the k-ε model[19,2] was chosen. This model adds two more differential equations: one for the turbulent kinetic energy, k, and one for the energy dissipation rate, ε. The first one governs the distribution of the local turbulent kinetic energy of the flow while the other governs the dissipation of the local energy. The two equations are,

$$\frac{\vartheta(\rho k)}{\vartheta t}+\frac{\vartheta(\rho uk)}{\vartheta x}+\frac{\vartheta(\rho vk)}{\vartheta y}+\frac{\vartheta(\rho wk)}{\vartheta z}=$$

$$\frac{\vartheta}{\vartheta x}(\Gamma_k\frac{\vartheta k}{\vartheta x})+\frac{\vartheta}{\vartheta y}(\Gamma_k\frac{\vartheta k}{\vartheta y})+\frac{\vartheta}{\vartheta z}(\Gamma_k\frac{\vartheta k}{\vartheta z})+S_k \qquad (7)$$

$$\frac{\vartheta(\rho\varepsilon)}{\vartheta t}+\frac{\vartheta(\rho u\varepsilon)}{\vartheta x}+\frac{\vartheta(\rho v\varepsilon)}{\vartheta y}+\frac{\vartheta(\rho w\varepsilon)}{\vartheta z}$$

$$=\frac{\vartheta}{\vartheta x}(\Gamma_e\frac{\vartheta\varepsilon}{\vartheta x})+\frac{\vartheta}{\vartheta y}(\Gamma_e\frac{\vartheta\varepsilon}{\vartheta y})+\frac{\vartheta}{\vartheta z}(\Gamma_e\frac{\vartheta\varepsilon}{\vartheta z})+S_\varepsilon \qquad (8)$$

where

$\Gamma_k = \frac{\mu_t}{Pr_k}$

$\Gamma_\varepsilon = \frac{\mu_t}{Pr_\varepsilon}$

$S_k = G_k - \rho\varepsilon + G_B$

$S_\varepsilon = \frac{\varepsilon}{k}[(G_k + G_B)(1+C_3R_f)C_1 - C_2\rho\varepsilon]$

$G_B = \mu_t g\frac{1}{\rho}\frac{\vartheta\rho}{\vartheta y}$

$$G_k = 2\mu_t\left[\left(\frac{\vartheta u}{\vartheta x}\right)^2+\left(\frac{\vartheta v}{\vartheta y}\right)^2+\left(\frac{\vartheta w}{\vartheta z}\right)^2\right]+$$

$$+\mu_t\left\{\left[\left(\frac{\vartheta u}{\vartheta z}\right)^2+\left(\frac{\vartheta w}{\vartheta x}\right)^2\right]+\left[\left(\frac{\vartheta w}{\vartheta y}\right)^2+\left(\frac{\vartheta v}{\vartheta z}\right)^2\right]+\left[\left(\frac{\vartheta u}{\vartheta y}\right)^2+\left(\frac{\vartheta v}{\vartheta x}\right)^2\right]\right\}$$

R_f = Richardson number

Pr_k = effective Prandtl number for k - equation = 1.0

Pr_ε = effective Prandtl number for ε - equation = 1.3

The turbulent viscosity is associated with the turbulent kinetic energy and dissipation rate by

$$\mu_t = C_\mu \rho k^2/\varepsilon \qquad (9)$$

Buoyancy modification through the use of the term, G_B, in the source term of the k-ε equation is essential for modeling compartment fire. In stable stratification, the term G_B increases the potential energy and reduces the turbulent mixing, while in unstable stratification, it enhances turbulence. As the shear layers for this problem are vertical, the Richardson number becomes very small and can be neglected. The source term for the ε equation can be written as,

$$S_\varepsilon = \frac{\varepsilon}{k}[(G_k + G_B)C_1 - C_2\rho\varepsilon] \qquad (10)$$

Based on this assumption, the empirical constant C_3 gets eliminated from the equation. The other empirical constants, C_1, C_2, C_μ are given in Table 1, together with the wall integration constant E and the von Karman constant κ which are used in the application of the boundary conditions.

Table 1.

C_1	C_2	C_μ	κ	E
1.44	1.92	0.09	0.4187	9.793

Boundary Conditions

The problem considered required the application of three different boundary conditions: wall, free and inlet.

Wall Boundary Conditions

The walls are considered no-slip and adiabatic. Therefore, on the wall

$$u = v = w = k = \varepsilon = 0, \quad q_{wall} = 0 \qquad (11)$$

The large gradient of viscosity next to the wall results in a large variation of the flow properties. As well, the Reynolds number can become small and the viscous effects can predominate over turbulence. Since most of the flow domain is surrounded by walls, the wall boundary conditions are very important. The accurate prediction of these properties requires a system of very fine meshes in the wall vicinity, resulting in rigorous calculations. An alternative approach is to use the *wall functions*, which provide a relationship between the grid point, the surface condition and the wall shear stressses. In this work, the logarithmic law proposed by Launder and Spalding[19] is used.

For the *momentum equations*, the velocity components on the wall are zero and the diffusion coefficient is given by:

$$y^+ \le 11.5 \rightarrow \Gamma_{ef} = \mu_l \qquad (12)$$

$$y^+ > 11.5 \rightarrow \Gamma_{ef} = \mu_l y^+ \kappa / \ln(Ey^+) \qquad (13)$$

where

$y^+ = \rho C_\mu^{0.25} \kappa^{0.5} y / \mu_l$

y = the normal distance of the grid point from the wall

For the *enthalpy equation*, the above equations take the following form,

$$y^+ \le 11.5 \rightarrow \Gamma_{ef} = \mu_l / Pr_l \qquad (14)$$

$$y^+ > 11.5 \rightarrow \Gamma_{ef} = \frac{\mu_l y^+ \kappa}{Pr_l}\left[\frac{\ln(Ey^+)}{\kappa} + 9\left(\frac{Pr_l}{Pr_t} - 1\right)\left(\frac{Pr_l}{Pr_t}\right)^{0.25}\right] \qquad (15)$$

For the *turbulent kinetic energy* equation, the diffusion coefficients defined for the momentum equations are used.

For the *energy dissipation* equation, wall functions are not used. The value of ε is calculated directly from the equation (after manipulation of the corresponding source term) as in[20],

$$\varepsilon = C_\mu^{\frac{3}{4}} k^{\frac{3}{2}} / (\kappa y) \qquad (16)$$

Inlet Boundary

For the inlet stream, the boundary conditions ensure that the temperature, pressure, and velocities in the inlet control volumes are equal to the ones defining the stream

$$u = u_{inl}, \; v = v_{inl}, \; w = w_{inl}, \; T = T_{inl}, \; P = P_{inl} \qquad (17)$$

and

$$k = \frac{3}{2}(u^*)^2 I^2, \qquad e = C_\mu^{0.75} k^{1.5} / l \qquad (18)$$

where

I = constant with values between 0.02 and 0.05

u^* = the area average inflow velocity

l = fraction of the inlet dimension

Free Boundary

On the free boundary, pressure is set equally to the ambient pressure and the derivative of the velocity components normal to the free surface is set to zero, permitting the flow to enter or leave the computational domain. For outflow, zero normal gradient conditions are imposed for all equations, while for inflow, the temperature, turbulent kinetic energy and dissipation rate are set equal to the corresponding ambient values (the equations constants were chosen as $I = 0.03$[16]). Therefore, for a boundary on a plane perpendicular to the x-axis, we have:

$$\frac{du}{dx} = \frac{dv}{dx} = \frac{dw}{dx} = 0, \quad P = P_{atm.}$$

for inflow and outflow (19)

$$\frac{dh}{dx} = \frac{dk}{dx} = \frac{d\varepsilon}{dx} = 0, \quad \text{for outflow} \quad (20)$$

$$\kappa = \kappa_{in}, \varepsilon = \varepsilon_{in} \; T = T_{in}, \quad \text{for inflow} \quad (21)$$

Initial Conditions

At the beginning of the simulation, all velocities are set to zero and temperature and pressure are set equal to the ambient conditions. The effective viscosity is assumed to be equal to the laminar one and turbulent kinetic energy and dissipation rate are set to small values ($1x10^{-9}$). To avoid divergence, the heat source was applied linearly with time, from zero up to its maximum value.

Numerical Procedure

The closed set of equations, given in the previous section, is solved numerically using the control volume formulation. The computational domain is divided into a number of rectangular cells, the control volumes. All scalar variables are located at the geometric centre of these control volumes, while velocity components are located at the control volume faces.

The governing equations are integrated over each control volume resulting in a set of integral balance equations. These are transformed into linear algebraic equations using the hybrid scheme for the interaction between convection and diffusion, and forward differencing for the unsteady term (central differencing was used for the spatial gradients of all variables). A fully implicit scheme for the time derivative was employed.

The resulting set of algebraic equations have the general form,

$$\left(S_\Phi = S_u + S_p \Phi_p\right) \quad (22)$$

where the source term has been linearized and k are all the neighboring points.

The velocity and pressure fields are linked together using the SIMPLE algorithm[21].

The solution sequence is as follows,

- Solve the momentum equations. Obtain new values for u, v, w.
- Solve the pressure equation. Obtain pressure corrections.
- Update u, v, w, and P using the pressure corrections.
- Solve enthalpy equation and obtain h.
- Calculate temperature T using the computed enthalpy h.
- Calculate density using the ideal gas equation (use T, P obtained before).
- Solve k-ε equations.
- Calculate new value for viscosity (based on p, k, ε).
- If error is larger than a specified convergence criterion, go back to the first step, if not proceed to the next time step.

The equations are solved using the tridiagonal matrix algorithm (TDMA)[21]. Each equation is solved using a number of inner block iterations, sequentially in all three directions (x, y, z). Under-relaxation is employed to improve convergence.

Results

To test the predictability of the model when used for compartment fire simulations, the predictions are compared with experimental data obtained by Steckler[22,23]. Steckler carried out a series of compartment fires using various configurations. These experiments have been also used as reference by other researchers[2,8,15].

The room simulated is 2.8 m square with a height of 2.18 m (Figure 1). Calculations were performed with both door and window openings. After several runs, the number of

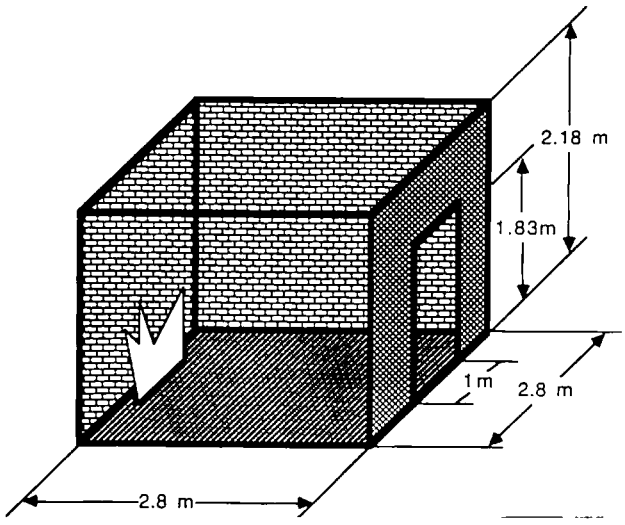

Figure 1: Three dimensional view of the fire compartment.

cells within tbe room chosen 20x20x10. To allow the complete development of flow at the opening, the computational domain was extended outside the room, resulting in a 34x34xl0 grid configuration. Because of the anisotropy of flow, a uniform grid system was used.

The heat release rate used in the experiments was 62.9 kW. To estimate the amount of heat lost by radiation and convection to the room boundaries, the heat convected by the gases out of the room was calculated and found equal to 60.9 kW. This value was then used in the numerical simulations.

The code is written in FORTRAN and calculations were performed on a Silicon Graphics Workstation. A time step of 1 second was chosen and 35 iterations were sufficient for each time iteration for convergence (with 2 inner block iterations for each equation). Steady state was achieved after 90 sec.

Comparisons with Experiments

Two sets of data were used: one for a room with a door and the second with a window.

Room with a Door

For this simulation, the door is located at the centre of the east wall, while the fire is located on the floor next to the west wall. The dimensions of the door are: height 1.83 m and width 0.74 m. Figures 2, 3 and 4 depict the temperature contours at 5, 10 and 60 seconds respectively. At time t = 5 s the hot plume moves up from the heat source, reaches the ceiling and starts moving along the ceiling towards the door. At t = 10 s, the hot gases reach the opening, while at t = 60 s, the flow is completely developed. At this time, the temperature at the heat source position is 1000 K. The hot gases exit from the upper part of the door going upwards, while the negative pressure developed inside the room draws cold air from outside through the lower part of the opening. The temperature fields for three orthogonal (y-z) planes (at the heat source, in the middle of the room, and outside the room) are shown in Figure 5. The symmetrical rise of the heated gases is clearly evident in the first plane, while at the middle of the room the two layers, cold and hot, are clearly distinguished. Figure 6 shows the velocity vectors for the middle x-y plane. At steady state (after 90 s) the flow rate of the hot gases out of the room was computed equal to 0.625 kg/s while the one measured in the experiments was 0.584 kg/s.

Figures 7 and 8 give a comparison between the predictions and experiments for the vertical temperature and velocity profiles at the door. The values used are average values at each height. The temperature near the floor is equal to the ambient temperature and remains constant for about half the height of the door. At the top of the door, the predicted and the experimental temperatures compare well. Near the bottom of the hot layer, the model seems to over-predict the temperatures. This is attributed to radiation losses from the hot gases that are not accounted for in the model. The predicted velocities are very close to the measured ones in both the inflow and the outflow regions. The predicted neutral plane is at almost the same height and the predicted maximum velocity is slightly smaller than the measured one.

Figure 9 shows a comparison between the predicted and experimental horizontal velocity profiles at the door at an elevation of

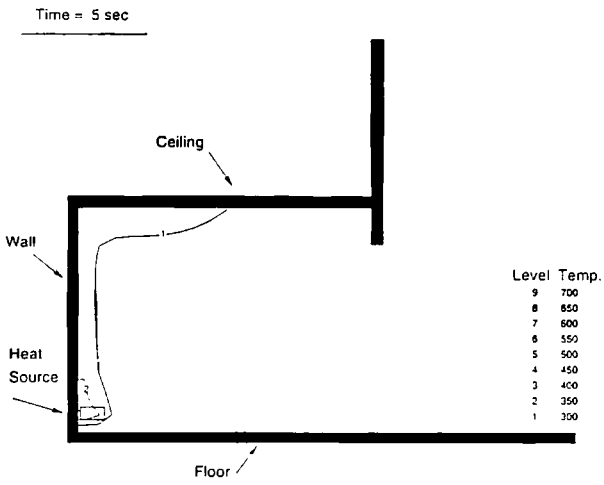

Figure 2: Temperature contours for the door case, with burner located at the inside corner at time t=5 sec (middle x-y plane).

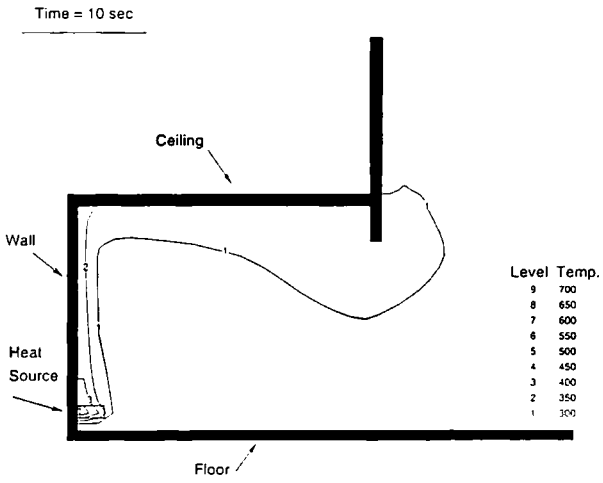

Figure 3: Temperature contours for the door case, with burner located at the inside corner at time t= 10 sec (middle x-y plane).

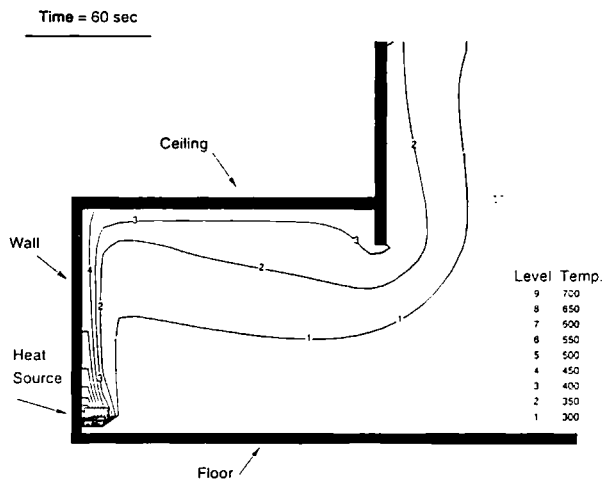

Figure 4: Temperature contours for the door case, with burner located at the inside corner at time t=60 sec (middle x-y plane).

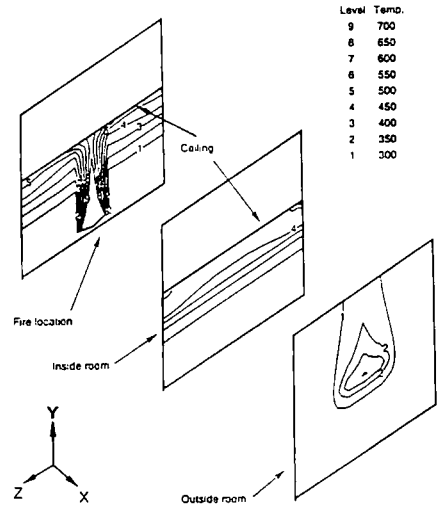

Figure 5: Temperature contours for the door case, with burner located at the inside corner for three z-y planes of the domain (t=60 sec).

1.7 m. The model fails to predict the velocity peaks near the door edges that are observed in the experimental data. This can be attributed to the fact that only 9 grid points in the horizontal planes were used at the door.

A comparison of the vertical temperature profiles 0.3 m inside the room and 0.3 m from the side-wall, is shown in Figure 10. The model can not predict accurately the high tmeperature gradients between the upper and lower layers.

Room with a Window

For this simulation, the room has a window opening, located at the centre of the east wall, 0.45 m from the floor. The dimensions of the window are: height 1.38 and width 0.74 m. The fire is located on the floor near the west wall and its intensity is 62.9 kW. At 60 s, the flow is fully developed and is depicted in Figure 11 (temperature field) and Figure 12 (velocity field) for the middle x-y plane. The mass flow rates through the opening are lower than for the door sce-

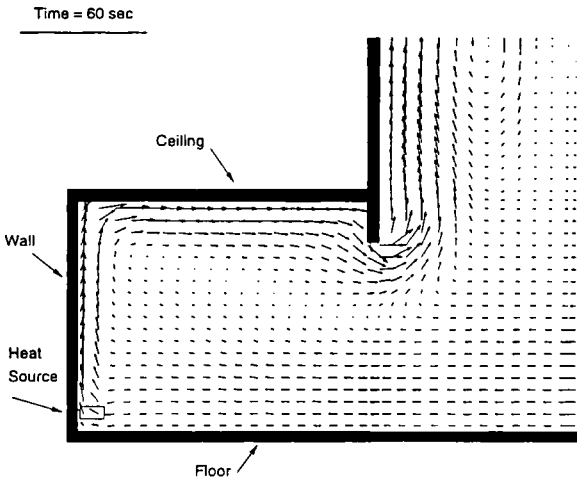

Figure 6: Velocity vectors for the door case, with burner located at the inside corner.

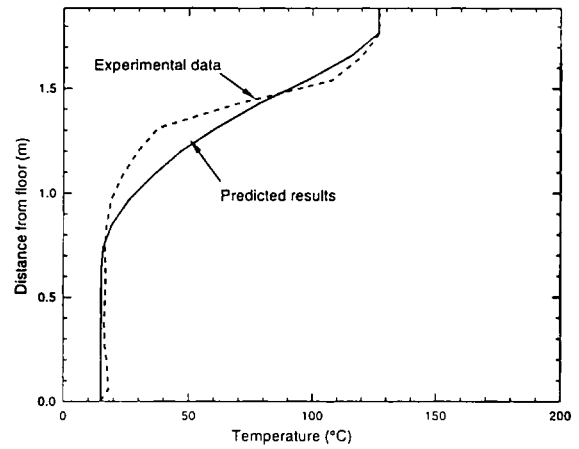

Figure 7: Comparison of predicted and experimental vertical temperature profiles at the door.

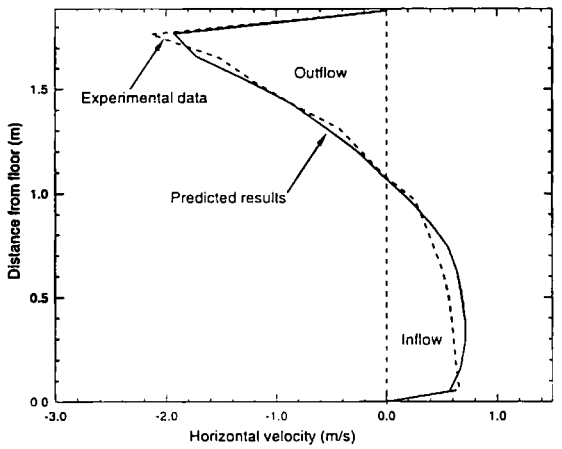

Figure 8: Comparison of predicted and experimental vertical velocity profiles at the door.

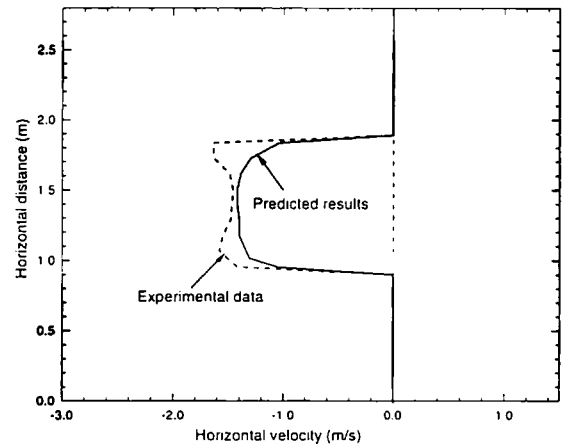

Figure 9: Comparison of predicted and experimental horizontal velocity profiles at the door.

nario, resulting in higher temperatures in the room. The mean flow rate in and out of the room is 0.494 kg/s.

Figures 13 and 14 give a comparison between the predictions and experiments for vertical velocity and temperature profiles at the window. The results are similar to the ones described for the door. The predicted velocity profiles are very close to the experimental ones, while the temperature profile is slightly different due to the lack of modeling radiation.

Other Simulations

A number of other simulations have been performed to investigate the effect of the fire location and obstacles in the room on the flow characteristics. For these simulations, the opening used was a door and the heat source was set equal to 60.9 kW.

Figures 15 and 16 show the temperature contours and velocity vectors, respectively, when the fire is located near the door. Although most of the hot gases leave the room, the

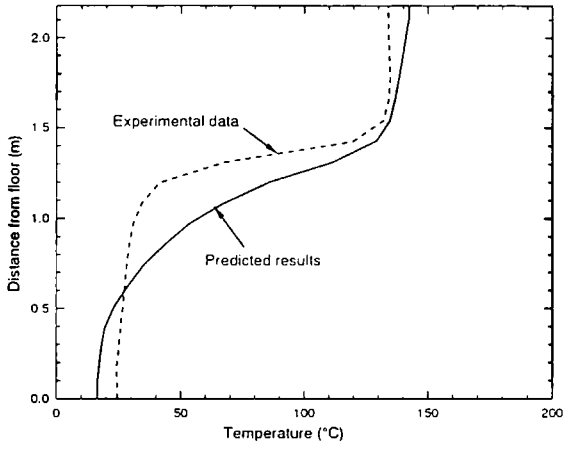

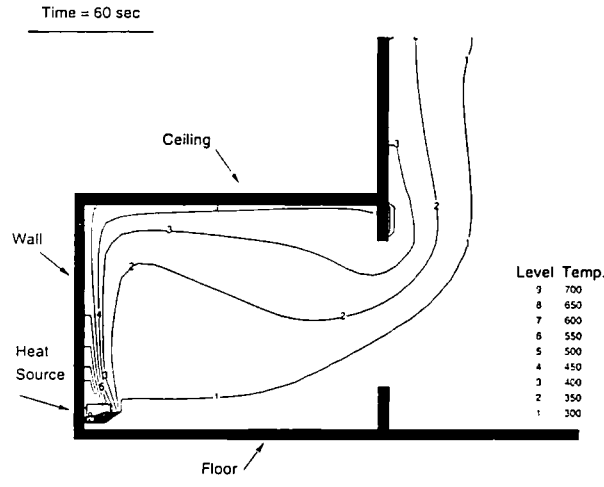

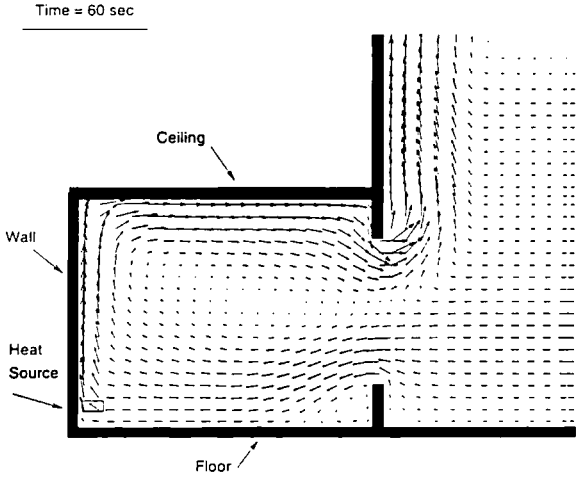

Figure 12: Velocity vectors for the window case (middle x-y plane).

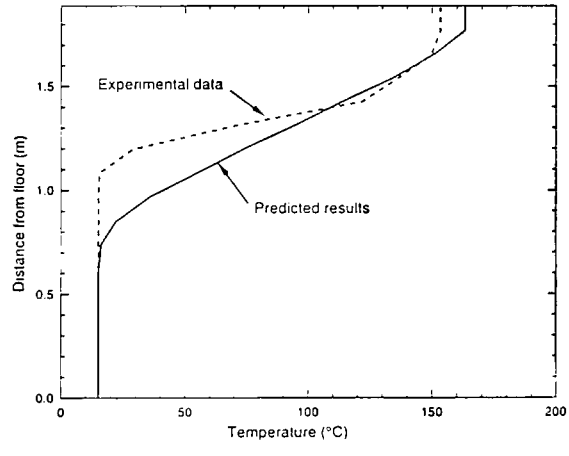

Figure 13: Comparison of predicted and experimental temperature profiles at the window.

hot layer in the room is thicker than when the fire is located at the far side from the door. This happens because the fire blocks the flow of fresh cool air into the room. For this case, comparison between experimentsand measurements for the temperature and velocity profiles at the door are shown in Figures 17 and 18.

Figure 19 shows a comparison of the velocity profiles with the fire located at three different positions inside the room (next to the west boundary, in the middle of the room and next to the door).

A simulation was performed to investigate the effect of internal objects on the flow inside the room. This configuration is of interest because it is encountered in many areas such as warehouses and engine rooms. Figure 20 and 21 show the velocity vectors and temperature contours of a 2-D simulation in which the obstacle is located in the room between the door and the fire. As it can be seen from the figures, the presence of the obstacle enhances the mixing of the two layers resulting in a thicker hot layer, hence an increase of the life-threatening conditions in the room. The mass flow rate

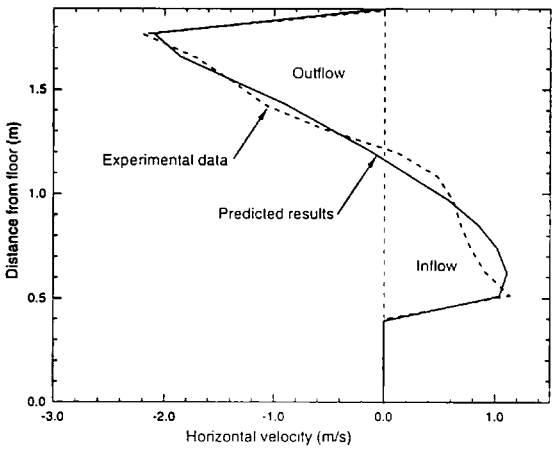

Figure 14: Comparison of predicted and experimental velocity profiles at the window.

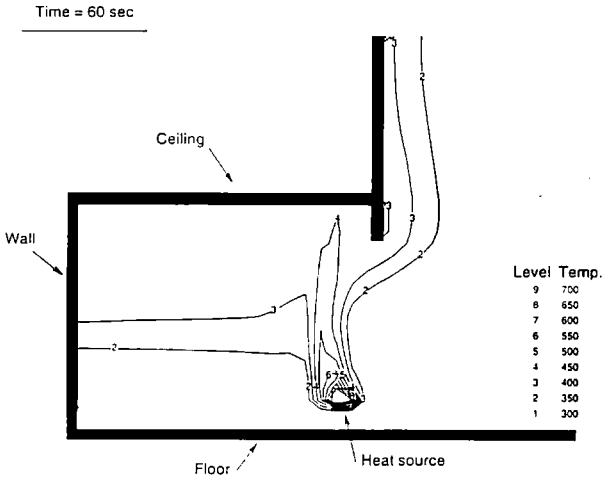

Figure 15: Temperature contours for burner located near the door.

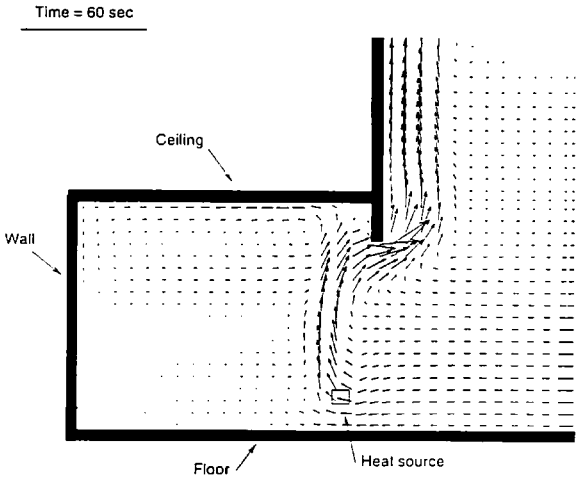

Figure 16: Velocity vectors for burner located near the door.

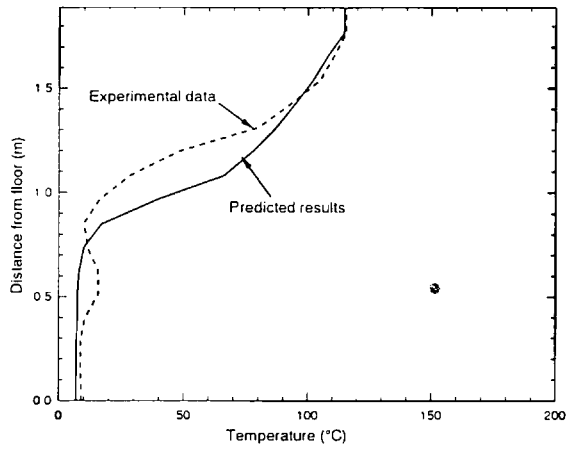

Figure 17: Comparison of predicted and experimental vertical temperature profiles at the door.

of air entering the room is less than when compared to the case of no obstacle by about 15 percent. The same problem was solved in 3-D and the results are shown in Figures 22 and 23 for two x-y planes, one next to the internal object and the other in the middle of the room. It can be observed that the cold air does not pass over the top of the object (as in the 2D case), but rather goes around it. Figure 24 shows the temperature contours for the same simulation for three z-y planes, one right at the fire location (next to the wall), one in the middle of the room (and therefore in the middle of the internal object) and one right outside the door. The figure shows that the flow is still symmetrical but the hot layer is thicker than that of the case without the obstacle.

SUMMARY

A field model is introduced, complete with the detailed description of its fundamental equations, turbulence model, boundary and initial conditions and solution algorithm. To demonstrate some applications, a number of simulations have been carried out to

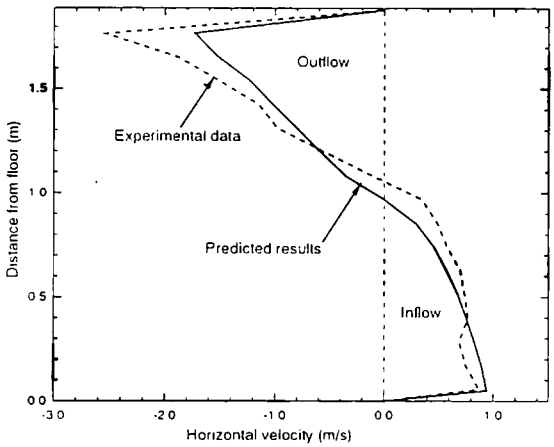

Figure 18: Comparison of predicted and experimental vertical velocity profiles at the door.

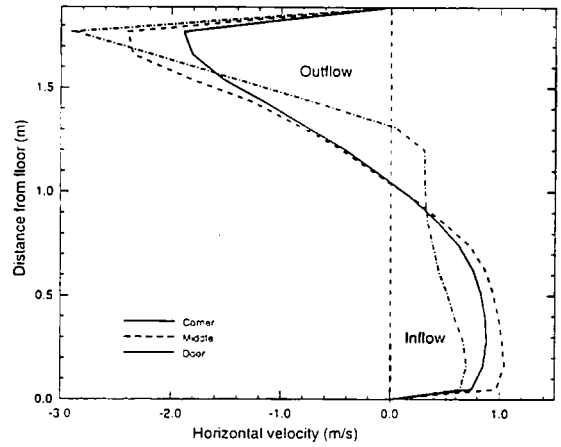

Figure 19: Predicted velocity profiles at the door for various fire locations.

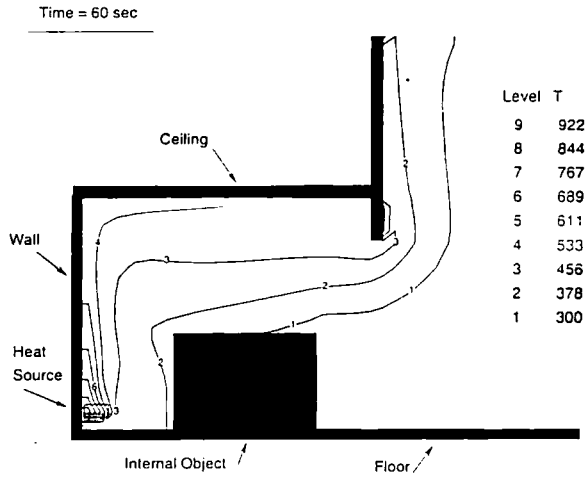

Figure 20: Temperature contours for door case with internal object and burner located at the inside corner.

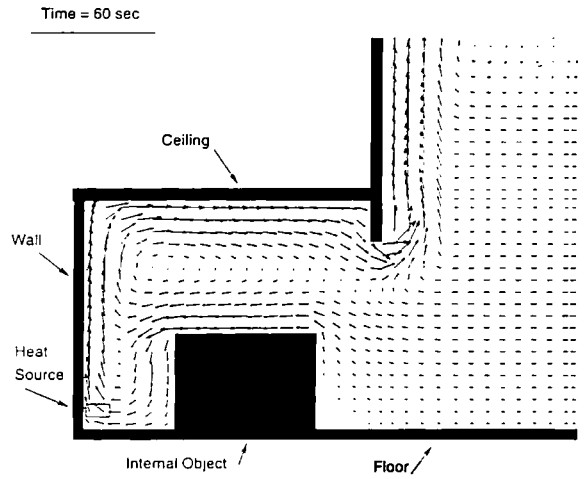

Figure 21: Velocity vectors for door case with internal object and burner located at the inside corner.

investigate the effect of the opening, fire position and internal objects. The predicted results show that:

- The model can predict compartment fires.
- The size of the opening affects the mass flow rate in and out of the room, which, in turn, affects the room temperature and the height of the hot layer.
- Fire location has a significant effect in the development of flow inside the room. The closer the fire is to the opening, the higher the room temperature.
- Internal objects may have a significant effect on the flow characteristics and the room temperature depending on their location and size.

Further work is required now to validate the model for a variety of fire sizes, compartment geometries, internal object positions and sizes and to model radiation and combustion. Future work will also include more comparisons to experimental data, especially for pool fires, fires in atria and rooms with multiple internal objects.

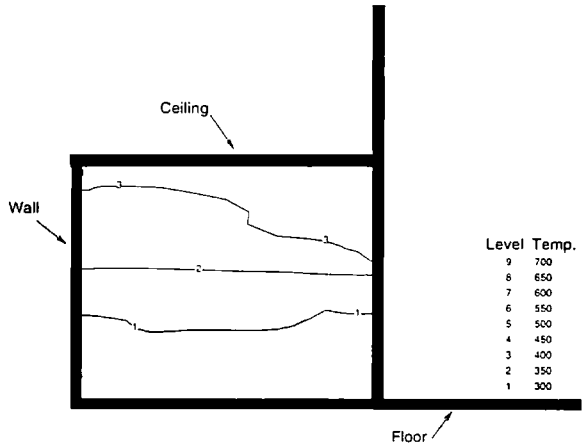

Figure 22: Temperature contours for door case with internal object and burner located on the floor near the middle of the west wall on two x-y planes. (a) Above, plane next to the obstacle. (b) Below, plane in the middle of the room.

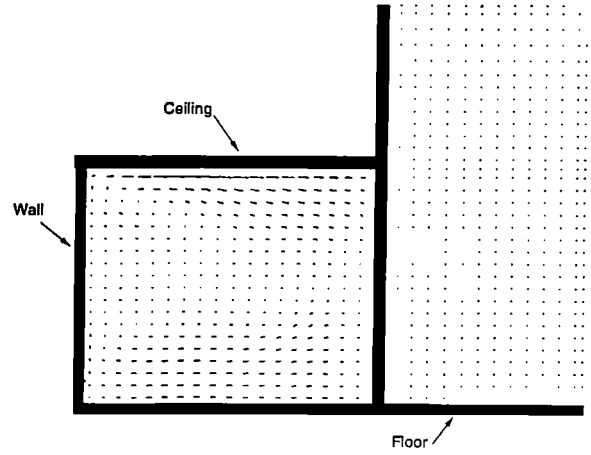

Figure 23: Velocity vectors for the door case with internal object and burner located on the floor near the middle of the west wall on two x-y planes. (a) Above, plane next to the obstacle. (b) Below, plane in the middle of the room.

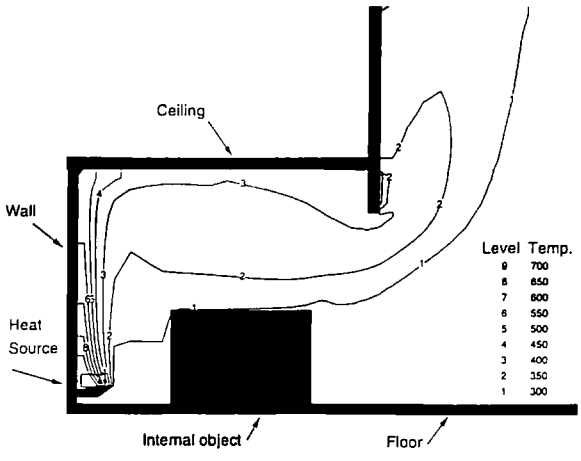

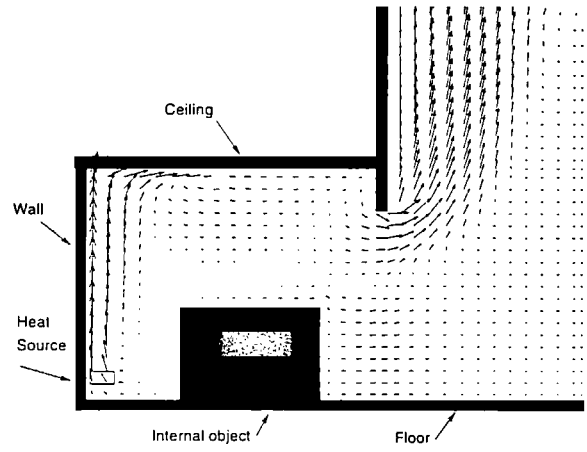

Figure 24: Temperature contours for door case with internal object and burner located on the floor near the middle of the west wall at three z-y planes.

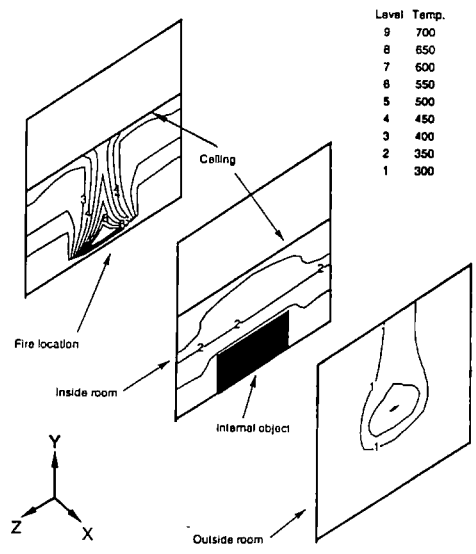

REFERENCES

1. Galea E., "On the Field Modeling Approach to the Simulation of Enclosure Fires," *Journal of Fire Protection Engineering,* **1,** No. 1, 1989, pp. 11–22, 1989.

2. Markatos N.C. and Cox G., "Hydrodynamics and Heat Transfer in Enclosures Containing a Fire Source," *Physico Chemical Hydrodynamics,* **5**, No. 1, 1984, pp. 53–66.

3. Cox G. and Kumar S., "Field Modeling of Fire in Forced Ventilated Enclosures," *Combustion Science and Technology*, **52**, pp. 7-23, 1987.

4. Cox G., Kumar S. and Markatos. N.C. , "Some Field Model Validation Studies," *Proceedings of the First International Symposium on Fire Safety Science,* 1985, pp. 159-171.

5. Kumar S., Gupta A.K., and Cox G., "Effects of Thermal Radiation on the Fluid Dynamics of Compartment Fires," *Proceedings of the Third International Symposium on Fire Safety Science,* 1991, pp. 34–354.

6. Ku A.C., Doria M.L., and Lloyd J.R. , "Numerical Modeling of Unsteady Buoyant Flows Generated by Fire in a Corridor." *Proceedings of the 16th Symposium (International) on Combustion,* 1976, pp. 1373-1384.

7. Yang K.T., Lloyd J.R., Kanury A.M., and Satoh K., "Modeling of Turbulent Buoyant Flows in Aircraft Cabins," *Combustion Science and Technology,* **39**, 1984, pp. 107-118.

8. Satoh K., "Three Dimensional Field Model Analysis of Fire-Induced Flow in an Enclosure with a Doorway Opening Comparison with NBS Fire Tests," Technical Report, Fire Research Institute of Japan, 1985.

9. Satoh K. and Kuwahara K., "A Numerical Study of Window to Window Propagation in High-Rise Building Fires," *Proceedings of the Third International Symposium on Fire Safety Science,* 1991, pp. 355–364.

10. Holen J., Hekkelstrand B., Evanger T, Byggstoyl S., and Magnussen B.F., "Finite Difference Calculation of Pool Fires and Jet Fires Offshore," *Proceedings of the Eurotherm Seminar,* 1990, pp. 24.1-24.10.

11. David W.D., and Wilkes, N.S., "A Finite Difference Method for the Computation of Fluid Flows in Complex Three Dimensional Geometries," Technical Report ACRE-R12342, HARWELL REPORT, 1987.

12. Morita M., Oka Y., and Hirota M., "Numerical Analysis and Computational Methods of Heat Flow in Fire Compartment," *Proceedings of the Second International Symposium on Fire Safety Science,* 1988, pp. 189-198.

13. Joh T., Mashige J., Yoshikawa T., and Sugawa O., "Numerical Simulation of a Compartment Fire from Burn-Up to Flashover," *Proceedings of the Third International Symposium on Fire Safety Science,* 1991, pp. 861-870.

14. Kaplan C.R. and Oran E.S., "A Numerical Study of Spontaneous Propane Ignition in a Partially Confined Volume," *Proceedings of the Third International Symposium on Fire Safety Science.* 1991, pp. 375-384.

15. Chow W.K. and Leung W.M., "Solid-Wall Boundary Effect on a Building Fire Field Model," *Combustion Science and Technology,* **71**, 1990, pp. 77-93.

16. Lai K.Y.M., "Turcom: A Computer Code for the Calculation of Transient, Multi-Dimensional, Turbulent, Multi-Component Chemically Reactive Fluid Flows: Part I: Turbulent, Isothermal and Incompressible Flow," Technical Report 1987/03, National Research Council of Canada.

17. Lai K.Y.M., "Turcom: A Computer Code for the Calculation of Transient, Multi-Dimensional, Turbulent, Multi-Component Chemically Reactive Fluid Flows: Part II: Compressible and Combustion Flow," Technical Report 1988/07, National Research Council of Canada, 1988.

18. Hadjisophocleous G.V. and Yakan A.C., "Computer Modeling of Compartment Fires," Technical Report 613, National Research Council of Canada, 1991.

19 Launder B.E. and Spalding D.B., "The Numerical Computation of Turbulent Flows," *Computer Methods in Applied Mechanics and Engineering*, 3, 1974, pp. 269–289.

20. Gosman A.D., Koosinlin M.L., Lockwood F.C., and Spalding D.B., "Transfer of Heat in Rotating Systems," Technical Report 76-GT-25, American Society of Mechanical Engineers, 1976.

21. Patankar S.V., *Numerical Heat Transfer and Fluid Flow,* McGraw Hill Book Company, 1980.

22. Steckler K.D., Quintiere J.G., and Rinkinen W.J., "Flow Induced by Fire in a Compartment," *Proceedings of the Nineteenth Symposium (International) on Combustion,* 1982, pp. 913-920.

23. Steckler K.D., Quintiere J.G., and Rinkinen W.J., "Flow Induced by Fire in a Compartment," Technical Report NBSIR 82-2520, National Bureau of Standards (US Department of Commerce), 1982.